THE MAGNESIUM PROBLEM IN SUPERALLOYS

A. Mitchell, M. Hilborn, E. Samuelsson and A. Kanagawa
Dept. of Metals and Materials Engineering
The University of British Columbia
Vancouver, B.C., Canada, V6T 1W5

INTRODUCTION

Magnesium in Superalloys

Magnesium is added to nickel-based superalloys to improve high temperature ductility. This property is important both from the manufacturing point of view, particularly in terms of open-die forgeability, and also from the in-service standpoint where rupture ductility is of primary importance. Further, it has been suggested that magnesium improves the low cycle fatigue strength[1,2].

Vacuum Induction Melting

A typical VIM cycle starts with the charging of either virgin raw materials or scrap. Following the pumping down, the furnace contents are melted. When the metal is entirely molten and the bath stable, desulphurizing or deoxidizing additions are made. Finally, reactive elements are added, and when the bath composition is correct the melt is cast[3].

Additions of aluminum and alkaline earth (AE) or rare earth (RE) metals decrease the activity and content of oxygen during the melting of a virgin heat. The increase of oxygen in the revert heat is probably due to pick-up from the refractories. In both cases, however the AE or RE additions help with the removal of oxygen-containing inclusions by the suggested mechanism of globurizing the alumina clusters[4].

Superalloys 1988
Edited by S. Reichman, D.N. Duhl,
G. Maurer, S. Antolovich and C. Lund
The Metallurgical Society, 1988

Calcium, magnesium, and rare earth metals are also strong desulphurizing agents. Figure 1 shows that the sulphur content can readily be reduced from ~ 150 ppm to ~ 10 ppm. The sulphide products deposit on the crucible walls. Hence, it is critical that the correct amount of desulphurizing agent can be predicted for each charge[4].

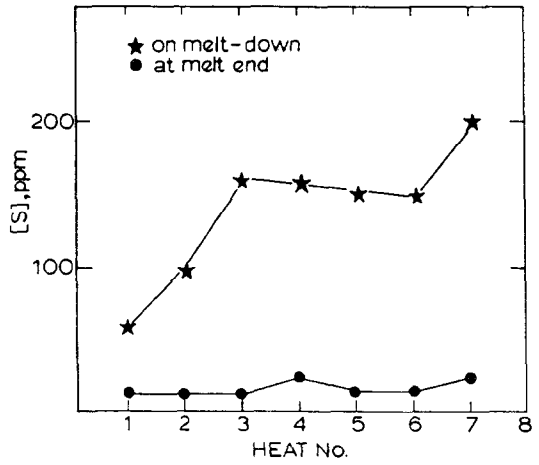

Figure 1: Reduction in melt sulphur content [S] over vacuum induction melting period[4].

Alexander[4] suggests that the removal of magnesium from VIM melts is controlled by liquid mass transfer while Fu et al[5] suggest that the controlling steps are liquid mass transfer and the evaporation reaction. However, the latter were forced, for lack of better data to assume that the activity of magnesium in nickel alloys is equal to the content. Clearly, additional data is required for more accurate analysis of the evaporation process during Vacuum Induction Melting.

Vacuum Arc Remelting

Fu et al[5] investigated the evaporation of magnesiuim from a nickel-base superalloy during VAR. They found that magnesium evaporates mainly from the electrode tip. It was suggested that the evaporation rate is limited by the transport of magnesium through the melt to the surface. However, the analysis of the problem is limited by lack of fundamental data.

Electro Slag Remelting

Ichihashi et al[6] investigated the ability of the ESR process to retain titanium, aluminum, and magnesium in the metal using different slag compositions. They show that increasing the contents of CaO and MgO will increase the content of magnesium in the ingot, as seen in Figure 2. They

also suggest that titanium or aluminum can be lost to the slag through following reactions:

$$3MgO + 2\underline{Al} \rightleftarrows Al_2O_3 + 3\,\underline{Mg}$$
$$2MgO + \underline{Ti} \rightleftarrows TiO_2 + 2\,\underline{Mg}$$

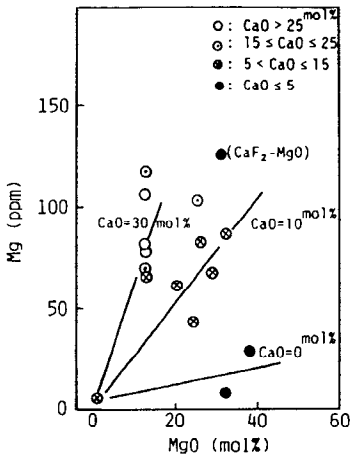

Figure 2: Effect of MgO content in the ESR slag on Mg content in produced ESR ingots[6].

Simultaneously, these reactions would increase the magnesium content in the alloy. It may be noted that proper control of the reactive element content is dependent on a delicate balance between slag and metal chemistry. Ichihasi[6] also found that magnesium can not be retained in the metal unless the slag is protected from air oxidation by an inert atmosphere, such as argon. Generally, the conclusions of Chen et al.[7] agree with those of Ichihashi[6].

Electron Beam Melting

The Electron Beam melting process has recently emerged as another alternative for superalloy refining[8]. The process, usually applied in the form of a Cold-Hearth Refining (EBCHR) furnace, offers more flexibility as to melting speed and ingot shape than the VAR process, since the heat source is independent of the charge material. However, the large area to volume ratio in the EBCHR process makes evaporation of alloying elements unavoidable. Hence, knowledge of the evaporation parameters of alloying elements is important if desired alloy compositions are to be produced.

Mitchell[9] and Herbertson[10] have discussed the evaporation of magnesium from superalloys during EBCHR refining. Mitchell[9] suggests that the

evaporation rate is controlled by the evaporation step and gives an evaporation rate constant of 2.5×10^{-7} m s^{-1} at 1700°C. On the other hand, Herbertson[10] claims that the evaporation rate is controlled by bulk mass transfer and gives a Langmuir evaporation rate constant of 1.5×10^{-1} m s^{-1} at 1700°C. It appears that Herbertson[10] has arrived at this value assuming an activity coefficient for magnesium in the liquid superalloy of unity. Using the suggested activity coefficient by Mitchell[9] of 10^{-3} for magnesium in liquid nickel, one arrives at an evaporation rate constant of 1.2×10^{-4} m s^{-1} at 1700°C and 3.6×10^{-4} m s^{-1} at 1700°C[11]. This would mean that magnesium evaporation is controlled by a combination of liquid mass transfer and evaporation. Hence, the activity coefficient is important in determining the rate-controlling step for evaporation during EBCHR refining.

Magnesium and Calcium in Nickel and Iron Alloys

The thermodynamic data of dilute iron solutions are better known than those for nickel solutions[12,13]. Therefore, when data for nickel alloys are lacking, many investigators apply those for iron as a best approximation. While this may be a valid approach for many systems, in the case of magnesium and calcium it is probably far from correct.

While the Mg-Fe phase diagram is incomplete, the binary systems Mg-Fe and Mg-Ni are essentially opposites[14,15]. Nickel-magnesium exhibits complete solubility in the liquid phase and two intermetallic compounds in the solid phase, whereas iron-calcium has an extensive miscibility gap in the liquid phase and no solid intermetallic phases. The situation is similar for the calcium-nickel and calcium-iron systems. The Ca-Fe phase diagram is even more tentative than the Mg-Fe diagram[16], but it is well known that the solubility of calcium in liquid iron is only 0.032 weight percent[17]. As in the nickel-magnesium system, nickel-calcium exhibits several solid intermetallic compounds and complete solubility in the liquid[18].

In terms of activity data one can then expect $\gamma_{Ca}/\gamma_{Mg} > 1$ in iron as in these systems the like atom attractions are stronger than the unlike atom attractions. In contrast, in nickel solutions γ_{Ca}/γ_{Mg} ought to be smaller than 1 as the intermetallic compounds indicate unlike atom attraction. This is also confirmed by Meysson and Rist[19] for nickel and iron-rich solutions containing calcium.

de Barbadillo[20] also discusses the influence of other alloying elements on the solubility of magnesium in nickel alloys. For instance, iron and chromium decreases the magnesium solubility. While insufficient data are available de Barbadillo manages to propose a tentative ternary liquid phase diagram for the Fe-Ni-Mg system. Figure 3 reproduces estimated activity data based on the limited data for the binary Ni-Mg system[21] and data for the system Ni-Fe-Mg[22].

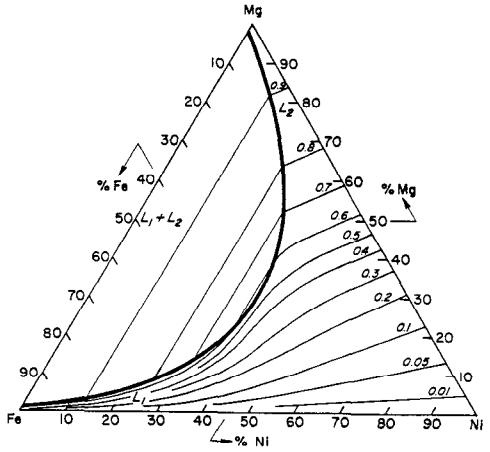

Figure 3: Estimated activity of magnesium in the Fe-Ni-Mg system[20].

Magnesium and Calcium

No experimental study of the deoxidation equilibria of Mg and Ca in nickel-base alloys has been found in the literature. Some work has been done on these elements in various iron-based solutions[23-26]. While these data may be useful in establishing deoxidation equilibria in nickel-base alloys the different solubility of Mg/Ca in the two solvents cannot be forgotten and must be taken into account in using the data of Tables I & II.

TABLE I: Deoxidation Equilibria in Iron Alloys

Deoxidation Reaction	log K	K	T (°C)	Ref.
$2Al + 3O \rightleftarrows Al_2O_3$ (s)		1.8×10^{13} 7.9×10^{13} 1.7×10^{13}	1600 1600 1600	28 27 23
$Ca + O \rightleftarrows CaO$		6.2×10^{5} 1.1×10^{6}	1600 1600	23 24,25
$Mg + O \rightleftarrows MgO$		5.5×10^{5}	1600	24,25

TABLE II: Deoxidation Equilibria in Nicel Alloys

Deoxidation Reaction	log K	K	T (°C)	Ref.
$2Al + 3O \rightleftarrows Al_2O_3$ (s)	$\frac{60795}{T} - 18.81$	4.48×10^{13}	1600	13
$Ca + O \rightleftarrows CaO$ (s)	$\frac{27959}{T} - 6.59$	2.16×10^{8}	1600	13
$Mg + O \rightleftarrows MgO$ (s)	$\frac{26009}{T} - 7.38$	3.2×10^{6}	1600	13

EXPERIMENTAL

The technique used to determine the activity coefficient of Mg in nickel-base alloys was the novel one of measuring vapour pressure with an atomic-absorption spectrophotometer. The experimental details are given in reference 29. The system was calibrated using both pure magnesium and Mg + Sn alloys. The equilibrium constant for the reaction:

$$Mg(g) \rightleftarrows [Mg]_{Ni}$$

was determined as:

$$\log K = 2.7 \text{ at } 1450°C$$

The Raoultian activity coefficient of Mg at 1450°C was found to be 1.2 (± 0.2) x 10^{-2}, with $e_O^{Mg} = -28$. The addition of Al, Fe and Cr did not substantially change these values in the concentration ranges up to 50% Ni, as shown in Figure 4.

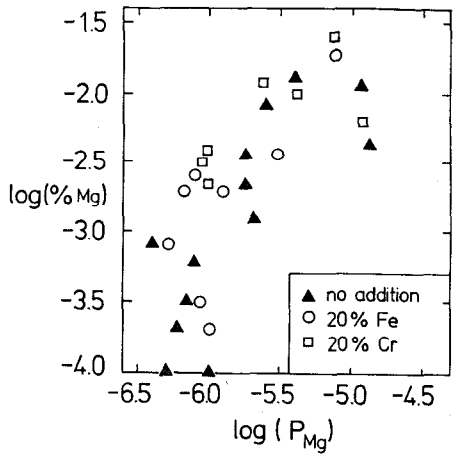

Figure 4: Comparison between data for alloys containing no major additions and alloys containing 20% Fe or 20% Cr.

Using the data given above we may compute the losses of Mg giving various process steps and compare these with the practically observed values. Since $[Mg]_{Ni}$ must also include that in equilibrium with MgS and MgO, we are able at the same time to estimate the levels of Mg in the three forms $[Mg]_{Ni}$, MgS and MgO at the various process stages.

The solubility product of MgO is extremely small, and in a system contained in pure MgO, we can assume that all oxygen is present as solid MgO. Therefore the maximum Mg present in this form is aprpoximately 10 ppm for a typical superalloy. In a VIM melt with an addition of 150 ppm Mg, and 10 ppm S, almost all the magnesium is $[Mg]_{Ni}$.

A comparison of Langmuir evaporation rates and bulk diffusion coefficients in VIM indicates that the latter controls the evaporation process. A surface depletion rate of 1.5×10^{-5} g $cm^2 s^{-1}$ is estimated for the melting conditions of a 5 tonne VIM melt of Inconel 718, equivalent to a bulk loss of 5 ppm Mg/min. This value accounts well for the "Mg-fade" observed during melting and casting.

Using the thermodynamic data generated above, we can also calculate the expected Mg contents of Inconel 718 melted by ESR, through a slag containing MgO, as shown in Figure 5. These values also compare well with observed practice and indicate that after ESR all the ingot Mg is as MgO or MgS.

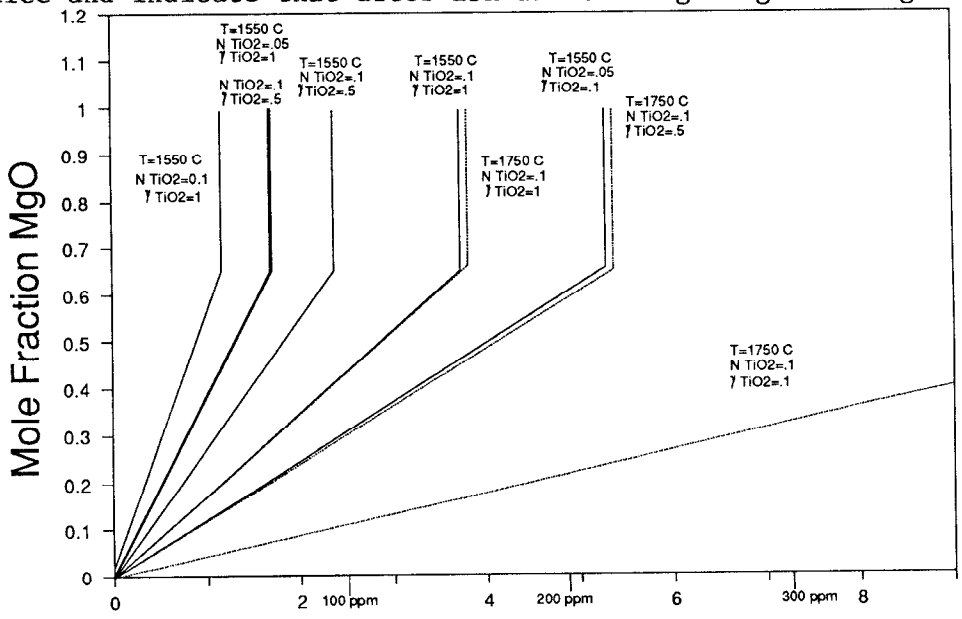

Figure 5: Calculated Equilibria for: $2[Mg] + (TiO_2) \rightleftarrows 2MgO + [Ti]$ for ESR slags based on $40CaF_2$: $30CaO$: $30Al_2O_3$ and alloy Inconel 718

The loss-rate of Mg from the same alloy melted by VAR may also be calculated. In an ingot of 500 mm ϕ, melted under typical industrial conditions, the loss rate is 100 ppm Mg/sec which indicates that all $[Mg]_{Ni}$ is removed by VAR, leaving only the equilibration of Mg from MgS and MgO as the ingot Mg content.

The solubility product of MgS is of considerable interest, as indicated by several workers, because of its impact on mechanical properties. Secondary precipitation of MgS has not yet been observed in Inconel 718, but the effect of Mg on mechanical properties must be through the elimination of grain-boundry S as MgS particles. The MgS carried in the liquid alloy system dissociates (Figure 6), but at room temperature it is likely tht all of the magnesium present in a VAR alloy is in the form of MgS or MgO. The same is true of EB-melted material. In view of the dissociation behaviour of MgS, and the high capacity for Mg removal in both EB and VAR, it is essential that the alloys processed this way should have a very low sulphur content. It appears that the dissociation of MgS will not permit the retention of more than 10 ppm sulphur as MgS at any content of Mg in Inconel 718 which is compatible with VAR or EB melting. It is to be noted that an intermediate de-sulphurizing step, such as ESR, will make this requirement possible. We also note that at a sufficiently-low sulphur content (<5ppm), adequate intermediate-temperature ductility may be obtained with magnesium contents at the residual levels of VAR or EB.

ACKNOWLEDGEMENTS

The authors are grateful for the support of the Teledyne Corp. (TRAP Programme) during the course of this work.

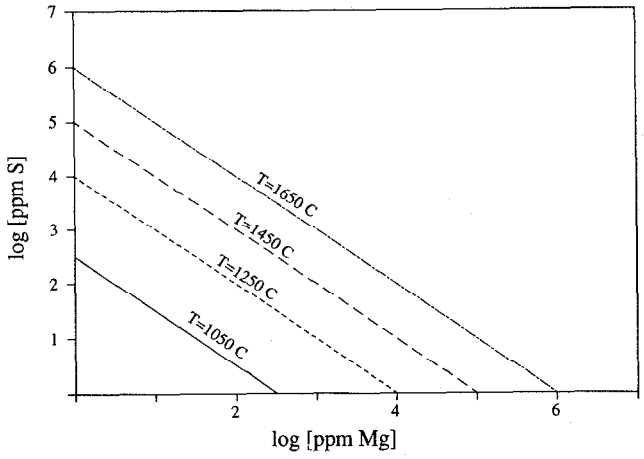

Figure 6: Reaction Equilibria for:
[Mg] + [S] = MgS(s) in Inconel 718

REFERENCES

1. C.T. Sims, W.C. Hagel, eds.: "The Superalloys", John Wiley & Sons Inc., 1972.

2. J.M. Moyer: Superalloys 1984, Prof. Fifth Int. Symposium on Superalloys, eds.: M. Gell et al., 1984, pp. 443-454.

3. R.S. Cremiso: "Melting" in "The Superalloys", eds.: Sims et al., John Wiley & Sons Inc., 1972, pp. 373-401.

4. J. Alexander: Material Science and Technology, Feb. 1985, V.1, pp. 167-170.

5. J. Fu, H. Wang, D. Wang, E.P. Chen: Proc. 7th ICVM, 1982, Tokyo, Japan.

6. H. Ichihashi, R. Baba, T. Ikeda: Proc. Vacuum Metallurgy Conf. 1984, pp. 75-82, Published by the Iron and Steel Soc., Eds.: G.K. Bhat, L.W. Lherbiev.

7. C.X. Chen, R.F. Gao, W.X. Zhao: 8th Intl. Conf. on Vacuum Metl., Linz, Austria, Sept. 30 - Oct. 4, 1985, V.2, pp. 1046-1052.

8. C. D'A. Hunt, J.H.C. Lowe, S.K. Harrington: Electron Beam Melting and Refining, Conf. Proc. Nov. 4-6, '85, Part I, pp. 58-70, Ed. R. Bakish.

9. A. Mitchell, K. Tagaki: Proc. Vacuum Metallurgy Conf. 1984, pp. 55-59, Published by the Iron and Steel Soc., Eds.: G.K. Bhat, L.W. Lherbier.

10. J. Herbertson: Conf. Proc.: Electron Beam Melting and Refining-State of the Art, 1986, pp. 19-29; Ed.: R. Bakish.

11. G.H. Geiger, D.R. Poirier: "Transport Phenomena in Metallurgy", Addison Wesley, 1973, pp. 560-567.

12. G.K. Sigworth, J.F. Elliott: Metal. Sci., V. 8, 1974, pp. 298-310.

13. G.K. Sigworth, J.F. Elliott, G. Vaughn, G.H. Geiger: Metallurgical Society of CIM, Annual volume featuring Molybdenum, 1977, pp. 104-110.

14. A.A. Nayeb-Hashemi, J.B. Clark, L.J. Swartzendruber: Binary Alloy Phase Diagrams, ed. T.B. Massalski, Am. Soc. Metl., 1986, p. 1076.

15. A.A. Nayeb-Hashemi, J.B. Clark: ibid, p. 1529.

16. W.G. Moffatt: "Handbook of Binary Phase Diagrams", Genium Publ. Corp., 1984.

17. D.L. Sponseller, R.A. Flinn: Trans. Met. Soc. AIME, V. 230, 1964, pp. 876-888.

18. W.G. Moffatt: ibid ref. 57, p. 628.

19. N. Meysson, A. Rist: Revue de Metallurgie, V. 62, 1965, pp. 1127-31.

20. J.J. de Barbadillo: "Magnesium and Calcium Treatment of Nickel-Base Alloys", Presented at American Vacuum Society Conf. 1975 (Available from the author at Inco Alloys Int., Huntington, W. VA).

21. N.G. Schmahl, P. Sieben: "The Physical Chemistry of Metallic Solutions and Intermetallic Compounds", Chemical Publishing Co. Inc., New York, 1960, pp. 268-290.

22. P.K. Trojan, R.A. Flinn: Trans. Am. Soc. Met., V. 54, 1961, pp.. 549-566.

23. S. Gustafsson, P-O. Mellberg: Scand. J. of Met., V. 9, 1980, pp. 111-116.

24. M. Joyant, C. Gatellier: "Influence d'une addition de calcium ou de magnesium sur la solubilite de l'oxygene et du soufre dans l'acier liquid", IRSID PCM-RE 1108, May 1984.

25. M. Nadif, C. Gatellier: ibid, PCM-RE 1108 Bis, June 1985.

26. N.A. Voronova: "Desulphurization of Hot Metal by Magnesium", Int. Magnesium Ass. and AIME, 1983, pp. 67-102.

27. A. McLean, H.B. Bell: J. Iron Steel Inst., Feb. 1965, pp. 123-130.

28. R.J. Fruehan: Met. Trans., V. 1, Dec. 1970, pp. 3403-3410.

29. Samuelsson, E., Magnesium in Liquid Nickel Solutions, Ph.D. Thesis, University of British Columbia, 1988.